MODELING BLAST-RELATED BRAIN INJURY

M. Nyein, A. Jérusalem, R. Radovitzky*
Massachusetts Institute of Technology
77 Massachusetts Ave, Cambridge, MA 02139

D. Moore
Defense and Veterans Brain Injury Center (WRAMC)
6900 Georgia Ave. NW, Washington, DC 20307

L. Noels
University of Liege
Chemin des chevreuils 1, B4000 Liege, Belgium

ABSTRACT

Recent military conflicts in Iraq and Afghanistan have highlighted the wartime effect of traumatic brain injury (TBI). While it is not clear why TBI has been so prominent in these particular conflicts, one reason may be that improvements in body armor have led to increased survivability of blasts. Closed traumatic brain injury covers a spectrum of central nervous system (CNS) injuries and mechanisms, but it is broadly characterized as mild (mTBI), moderate, or severe TBI, with mTBI occurring most frequently. Blunt, ballistic, and blast effects may all contribute to CNS injury, but blast in particular has been suggested as a primary cause of military TBI. Little is currently known about the effects of blasts on the CNS; injury thresholds have not been established, and even direct transmission of the non-linear shock wave into the intra-cranial cavity and brain is disputed. In this study, we demonstrate the potential for a blast shockwave to directly affect the CNS using coupled computational fluid-solid dynamics simulation. The model includes a complex finite element model of the head and intracranial contents. The effects of threshold and lethal blast lung injury were compared with concussive impact injury using the full head model.

1. Introduction

Current military operations in Iraq (Operation Iraqi Freedom) and Afghanistan (Operation Enduring Freedom) have brought into sharp focus military-related traumatic brain injury (TBI). TBI is a significant cause of death and morbidity in the 0 to 40-year-old range with a huge direct and indirect economic impact through the burden of care imposed on family members and society at large (Brazarian et al., 2005; Bruns and Hauser, 2003). Although blasts have been suggested as a primary cause of military TBI, little is currently known about the effects of blasts on the CNS. Blast effects on some biological tissues, such as the lung, are documented in terms of injury thresholds, but this is not the case for the CNS. Even direct transmission of the non-linear shock wave into the intra-cranial cavity and brain is disputed, with one suggested mechanism of potential CNS injury being indirect transmission of the blast compression wave via the cerebral vasculature. There is no current experimental evidence that blast waves per se alter the CNS injury cascade of TBI compared to blunt injury.

A blast wave is a pressure wave of finite amplitude resulting from an atmospheric explosion that releases a large amount of energy in a short period of time. In addition to the blast wave, the chemical energy of the explosion is released into thermal, electromagnetic, and possibly into kinetic energy of solid fragments and surrounding material (Strehlow and Baker, 1976). The non-linear shock wave represents a large discontinuous increase in pressure and density in the air which propagates radially from the source of the explosion with the potential to cause large loading transients. Importantly, an explosive event is stochastic with the characteristics of a three-dimensional complex flow field that may be altered by ambient conditions and environmental boundaries that can result in wave reflections and up to eight-fold field intensification (Cullis, 2001; Kambouchev et al., 2007). A free field blast wave can be most simply described by the idealized Friedlander waveform with a rapid rise to the peak pressure, exponential fall-off of the overpressure, together with a relatively prolonged underpressure, resulting in a combination of compressive and tensile components as it propagates through a material (Taylor, 1950; von Neumann, 1943). The interaction of a blast wave with a material either biological or non-biological results in the development of stress waves which have longitudinal, shear (transverse), and shear (Rayleigh) wave components (Kolsky, 1963). Development of a shear wave where the direction of particle motion is orthogonal to the direction of wave propagation results in material shear stresses that may have a different pathological effect on the anisotropic structures of the brain, especially white matter tracts.

Coupling of the nonlinear blast shockwave into

Report Documentation Page

Form Approved
OMB No. 0704-0188

Public reporting burden for the collection of information is estimated to average 1 hour per response, including the time for reviewing instructions, searching existing data sources, gathering and maintaining the data needed, and completing and reviewing the collection of information. Send comments regarding this burden estimate or any other aspect of this collection of information, including suggestions for reducing this burden, to Washington Headquarters Services, Directorate for Information Operations and Reports, 1215 Jefferson Davis Highway, Suite 1204, Arlington VA 22202-4302. Respondents should be aware that notwithstanding any other provision of law, no person shall be subject to a penalty for failing to comply with a collection of information if it does not display a currently valid OMB control number.

1. REPORT DATE **DEC 2008**	2. REPORT TYPE **N/A**	3. DATES COVERED **-**
4. TITLE AND SUBTITLE **Modeling Blast-Related Brain Injury**		5a. CONTRACT NUMBER
		5b. GRANT NUMBER
		5c. PROGRAM ELEMENT NUMBER
6. AUTHOR(S)		5d. PROJECT NUMBER
		5e. TASK NUMBER
		5f. WORK UNIT NUMBER
7. PERFORMING ORGANIZATION NAME(S) AND ADDRESS(ES) **Massachusetts Institute of Technology 77 Massachusetts Ave, Cambridge, MA 02139**		8. PERFORMING ORGANIZATION REPORT NUMBER
9. SPONSORING/MONITORING AGENCY NAME(S) AND ADDRESS(ES)		10. SPONSOR/MONITOR'S ACRONYM(S)
		11. SPONSOR/MONITOR'S REPORT NUMBER(S)

12. DISTRIBUTION/AVAILABILITY STATEMENT
Approved for public release, distribution unlimited

13. SUPPLEMENTARY NOTES
See also ADM002187. Proceedings of the Army Science Conference (26th) Held in Orlando, Florida on 1-4 December 2008, The original document contains color images.

14. ABSTRACT

15. SUBJECT TERMS

16. SECURITY CLASSIFICATION OF:			17. LIMITATION OF ABSTRACT	18. NUMBER OF PAGES	19a. NAME OF RESPONSIBLE PERSON
a. REPORT **unclassified**	b. ABSTRACT **unclassified**	c. THIS PAGE **unclassified**	**UU**	**8**	

Standard Form 298 (Rev. 8-98)
Prescribed by ANSI Std Z39-18

biological tissue results in significant energy deposition at high strain rates in fractions of milliseconds. The relative amount of energy deposition will be most simply dependent on the distance from the blast source (inverse cube law) together with the high strain rate tissue material properties. Recent data suggests that tissue shear response may exhibit differing states across the range of high strain rates as determined by Kolsky bar experiments. Similar experiments indicated that the bulk modulus, while non-linearly related to strain rate, did not exhibit more than one state (Saraf et al., 2007).

The propagation of stress waves in the brain and their relation to TBI have been studied via simulation under impact loading (e.g., Zhang et al., 2004; Willinger and Baumgartner, 2003). However, due to the characteristics of blast waves, it is expected that the loading transients under blast conditions may involve much shorter chacteristic time scales, leading to higher strain rates than seen under impact conditions. This may set in motion deformation mechanisms of tissue response that are not operative under impact conditions, which may, in turn, lead to a differing spectrum of blast-related brain injury.

The purpose of this paper is to develop a full head model and simulation of the fluid-solid interaction with a blast shockwave and to interpret these events with reference to the Bowen curves, which give the estimated tolerance to a single blast at sea level for a 70-kg human oriented perpendicular to the blast (Bowen et al., 1968). Estimates from the Bowen curves suggest that the threshold for unarmored parenchymal lung injury at standoff of 0.6 m is 80 psi or 5.45 atm, while 400 psi or 27.21 atm results in 1% survival from lung injury. 250 psi or 17.01 atm is the LD_{50} (lethal dose, 50%) with approximately 50% survival from lung injury (Bowen et al., 1968).

In order to examine and compare the effects of blast shock waves on the human head, simulations were run with a full head mesh in three different contexts: (1) a blast with overpressure of 5.2 atm or threshold lung injury, equivalent to a free air explosion of 0.0648 kg TNT at a 0.6 m standoff distance;(2) a blast with overpressure of 18.6 atm or near the LD_{50} of lung injury survival, equivalent to a free air explosion of 0.324 kg TNT at a 0.6 m standoff distance; and (3) an impact between a head traveling at 5 m/s and a stationary, immovable boundary. The overpressures for the two blast simulations were selected based on the Bowen curves(Bowen et al., 1968). In the impact simulation, it was determined that the impact velocity should be 5 m/s in order to result in concussive injury, based on comparable impact studies in the literature (Casson et al., 2008; Zhang et al., 2004).

2. Methods

High resolution T1 MR images were downloaded from the Montreal Neurological Institute at an isotropic voxel dimension of 1 x 1 x 1 mm (Collins et al., 1998). These images were merged with a bone windowed CT of the head allowing skull reconstruction using a mutual information algorithm. The resulting volume set of images was then segmented by hand into topological closed regions of interest using Amira and then exported as VRML files. These files were imported into ICEMCFD, and unstructured finite element meshes were formed using Octree and Delaunay tetrahedral mesh generation algorithms. The meshes were further refined by isolation of poorly meshed areas and poorly shaped tetrahedra prior to running the computational fluid-solid dynamics code (Deiterding et al., 2006). It was found that meshes with fewer than 700,000 elements were too coarse to describe the intricate geometry and topology of some anatomical structures of the human head deemed relevant for blast injury analysis. Previous computational models have been reported in the literature having a maximum of 314,500 elements (Zhang et al., 2001).

In order to balance the mesh resolution and computational requirements, a mesh with 808,766 elements was used in the simulations. Meshes of higher definition will be evaluated in future work in combination with higher-fidelity constitutive models and properties of tissue reponse. The computational model differentiates 11 distinct structures characterized by mechanical function rather than physiology: ventricular cerebrospinal fluid, peri-ventricular glia, white matter, gray matter, eyes, venous sinuses, subarachnoid cerebrospinal fluid, air sinuses, muscle, skin and fat, and diploic skull bone.

3. Material Models

The constitutive response of brain tissue encompasses a variety of complex mechanisms including nonlinear viscoelasticity, anisotropy, and a strong rate dependence (Velardi et al., 2006; Shen et al., 2006). Several investigations have focused on characterizing this response experimentally and on developing a variety of constitutive models capturing this behavior (e.g., Miller and Chinzei, 2002; Prange and Margulies, 2002). Owing to the complexities and inherent variability associated with biological tissue, there is usually significant uncertainty in quantifying tissue response. In consideration of these limitations, computational models have usually favored simpler (i.e. elastic) models with few parameters that can be quantified with less uncertainty, instead of more sophisticated models with many parameters that are harder to estimate. In

the impact TBI modeling work, isotropic elastic models have been used for the volumetric response while linear viscoelastic effects have been considered in the shear response via a time-dependent shear modulus evolving from the instantaneous to the long-term value (Belingardi et al., 2005; Willinger and Baumgartner, 2003; Zhang et al., 2001). The relaxation times involved are on the order of tens to hundreds of milliseconds or higher. It is therefore reasonable to expect that deferred deformation or stress relaxation due to viscoelastic effects play a secondary role under blast loading, where the characteristic times seldom, if ever, exceed a few milliseconds.

On this account, and as a first approximation, we have adopted a simplified constitutive modeling strategy emphasizing the effects pertinent to blast conditions, specifically the description of the pressure wave propagating through the brain via a suitable equation of state. To this end, the volumetric response of brain tissue has been described by the Tait equation of state with parameters adjusted to fit the bulk modulus of the various tissue types. The deviatoric response has been described via a large-deformation, neo-Hookean elastic model with properties adjusted to fit reported values of the instantaneous shear modulus. The Mie-Gruneisen/Hugoniot equation of state was used to describe the volumetric response of the skull. The constitutive properties of the tissues were determined from a literature review.

3.1 Mie-Gruneisen/Hugoniot Equation of State

The shock response of many solid materials is well described by the Hugoniot relation between the shock velocity U_s and the material velocity U_p of the simple form (D.S. Drumheller, 1998; M.A. Meyers, 1994; Zel'dovich and Raizer, 1967):

$$U_s = C_0 + sU_p \tag{1}$$

In this expression, C_0 and s are material parameters that can be obtained from experiments. Here the values for C_0 and s are the same as those used for the skull in Taylor and Ford (2006). By considering Equation (1) and conservation of mass and momentum in a control volume at the shock front, the final pressure can be calculated explicitly as a function of the Jacobian behind the shock front J_H and the reference density ahead of the shock ρ_0 (D.S. Drumheller, 1998; M.A. Meyers, 1994; Zel'dovich and Raizer, 1967):

$$P_H = \frac{\rho_0 C_0^2 (1 - J_H)}{[1 - s(1 - J_H)]^2} \tag{2}$$

where J_H is related to the density ρ_H, the specific volume V_H, or the deformation gradient tensor F_H, defined behind the shock front, by:

$$J_H = \frac{\rho_0}{\rho_H} = \frac{V_H}{V_0} = det(F_H) \tag{3}$$

The relation Equation (2), called the shock Hugoniot, relates any final state of density to its corresponding pressure. The deformation path taken by the material between the initial state (P_0, V_0) and the final state (P_H, V_H) is then defined by the Rayleigh line: a straight line in the (σ_1, V) plot, where σ_1 is the axial stress in the shock direction (D.S. Drumheller, 1998; M.A. Meyers, 1994). The parameters used in the simulations are given in Table 1.

Structure	$\rho(kg/m^3)$	$E(Pa)$	ν	C_0	S
Skull	1412	6.5e9	0.22	1.85e3	0.94

Table 1: Material Parameters for the Skull

3.2 Tait Equation of State

The Tait equation of state, which is commonly used to model fluids, is given by (Thompson, 1972):

$$p = B[(\rho/\rho_0)^{\Gamma_0+1} - 1] \tag{4}$$

where B and Γ_0 are constants. The Tait equation of state was selected to describe the volumetric response of all head structures except the skull because the remaining structures largely consist of water. To obtain the necessary parameters, Γ_0 was taken to be the value for water, 6.15, appropriate bulk modulus values K were selected from the literature, and B was computed for each structure using the relation:

$$K_0 = B \times (\Gamma_0 + 1) \tag{5}$$

3.3 Deviatoric Elasticity

In addition, all of the structures were assumed to obey an elastic deviatoric behavior. To this end, the equilibrium stress-strain relation was extended to include the elasticity of the material in shear, with the result (Cuitino and Ortiz,1992; Ortiz and Stainier, 1999):

$$\sigma^B = -PI + J^{-1} F^e [\mu (log\sqrt{C^e})^{dev}] F^{eT} \tag{6}$$

where $C^e = F^{eT} F^e$ is the elastic Cauchy-Green deformation tensor, $log\sqrt{C^e}$ is the logarithmic elastic strain, μ is the shear modulus, and the pressure P follows from the equations of state defined in Equations (2) and (4). Explicit formulae for the calculation of the exponential and logarithmic mappings, and the calculation of their first and second linearizations, has been given by Ortiz et al. (2001). For the simulations, values of μ were selected from the literature. These values are listed in Tables 1 and 2.

Structure	$\rho(kg/m^3)$	K (Pa)	B	Γ_0	$\mu(Pa)$
Ventricle	1040	2.19e9	3.063e8	6.15	2.25e4
Glia	1040	2.19e9	3.063e8	6.15	2.253e4
White Matter	1040	2.19e9	3.063e8	6.15	2.253e4
Gray Matter	1040	2.19e9	3.063e8	6.15	2.253e4
Eyes	1040	2.19e9	3.063e8	6.15	2.253e4
Venous Sinus	1040	2.19e9	3.063e8	6.15	2.013e4
CSF	1040	2.19e9	3.063e8	6.15	2.253e4
Air Sinus	1040	2.19e9	3.063e8	6.15	2.253e4
Muscle	1100	3.33e6	4.662e5	6.15	3.793e4
Skin/Fat	1040	3.47e7	4.866e6	6.15	5.880e6

Table 2: Material Parameters for Head Structures

4. Simulation Details

The two blast fluid-solid interaction simulations were run on 14 processors for the solid and 6 processors for the fluid, with two levels of subdivision allowed for the fluid. The lower region of the head was fixed in order to avoid the blast engulfing the bottom of the head, where the neck would ordinarily be located. The solid-only impact simulation was run on 20 processors.

5. Results

5.1 5.2 atm Simulation

Figures 1(a)-(f) illustrate the propagation of the compressive blast wave through the coronal sections of the head in the 5.2 atm simulation. The blast wave is incident on the right temporal region. The compressive wave is seen propagating through the cranial cavity from the right to the left with some minor reflection from the left side of the cavity, leading to a pocket of concentrated pressure in the skull on the right side of the head.

The maximum tensile and compressive pressures were extracted and plotted for each time step for each of the 11 distinct structures. These curves are given in Figures 2(a)-(f) for the blast and impact simulations. In the 5.2 atm simulation, the maximum compressive pressure reached was 6.5 MPa at 0.00045 s, and the maximum tensile pressure reached was 0.89 MPa at 0.00048 s. It is evident from the curves that the various structures experienced different time courses and different pressure intensities. The highest compressive pressures were experienced by the skull, muscle, and subarachnoid CSF, while the highest tensile pressures were experienced by the air sinuses, gray matter, subarachnoid CSF, skull, and white matter. In this simulation, the nodes that experienced the highest pressures were all located on the right side of the head, in the concentrated pocket of stress created from the reflection of the blast wave from the left side of the head.

5.2 18.6 atm Simulation

At the LD_{50} blast wave overpressure of 18.6 atm, the compressive propagation is seen in Figure 3 with generation of differential stresses as the wave propagates. Wave reflection is more apparent at this overpressure as seen in the multiphasic curves of Figures 2(c) and (d). The simulation reached a maximum compressive pressure of 39 MPa at 0.00042 s in the skull and muscle and a maximum tensile pressure of 4.5 MPa at 0.00041 s in the skull and gray matter. High compressive pressures were experienced by the skull, muscle, subarachnoid CSF, gray matter, and skin/fat material elements. The skull experienced peak compressive pressure first, followed by the subarachnoid CSF and muscle, and then gray matter. High tensile pressures were experienced by the skull, subarachnoid csf, gray matter, and white matter. Compared to the 5.2 atm simulation, the 18.6 atm simulation experienced pressures that were 4-6 times higher than those experienced in the 5.2 atm simulation, and the pressures and stresses peaked earlier in the 18.6 atm simulation. The locations in the head that experienced the highest stresses were very similar in both the 5.2 atm and 18.6 atm simulations.

5.3 Impact Simulation

The 5 m/s impact simulation ran to .000634 s, reaching a maximum compressive pressure of 27.2 MPa and a maximum tensile pressure of 7.1 MPa. The impact was delivered in the mid-coronal plane in a lateral direction, from left to right. Significant differences are seen between blast and impact injury, specifically in the monotonic form of the impact compression and tension curves.

High compressive pressures were experienced by the skull, subarachnoid CSF, muscle, skin/fat, and gray matter, with the highest compressive pressure being experienced by the skull. High tensile pressures

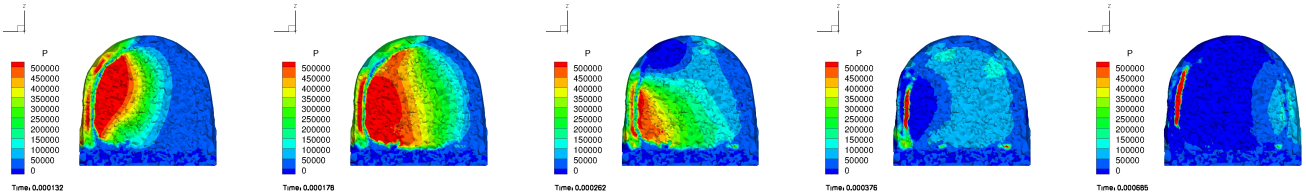

(a) **0.000132 s** (b) **0.000178 s** (c) **0.000262 s** (d) **0.000376 s** (e) **0.000685 s**

Figure 1: Propagation of blast compressive wave through cranial cavity in 5.2 atm simulation, viewed through mid-coronal plane at 0.132-0.685 ms. The propagation of the blast wave is from left to right in the external observer frame of reference. Scale is from 0 to 500 kPa.

were experienced by the skull, muscle, skin/fat, and gray matter, again with the highest tensile pressure being experienced by the skull. The magnitudes of the maximum pressures reached in the impact simulation are comparable to the maximum pressures reached in the 18.6 atm simulation, suggesting that blasts that would result in 50% lethality due to unarmored parenchymal lung injury would lead to concussive injury in the brain.

CONCLUSIONS

The use of personal protective equipment (PPE), particularly body armor, is considered to be protective against lethal blast and fragmentation lung injury. The goal of this work was to use the standardized Bowen curves for threshold and 50% lethal lung injury to examine the effects of similar exposures on the head and to compare them with impact decelerations such as those often seen within sports concussions (Zhang et al., 2004). The analysis indicates that injury from a blast resulting in 50% lethal unarmored lung injury is associated with impact injury that may result in concussion. The American Academy of Neurology grades concussions from 1-3, with grade 3 implying a loss of consciousness and grades 1 and 2 implying transient confusion (American Academy of Neurology, 1997). In the military context such transient confusion may lead to a loss of situational awareness within the combat context, with potentially devastating results. These results need to be experimentally validated and are best considered by regarding TBI to occur across a strain-rate continuum with impact injury occurring at lower strain rates, ballistic injury at intermediate to higher strain rates, and blast injury at the highest strain rates (Moore et al., 2008). Such validation requires both experimental measurement but also appropriate models of tissue constitutive properties across the strain-rate continuum. The constitutive models used in the current simulations - the Tait and Mie-Grueneisen/Hugoniot equations of state - while likely to be refined by further experimental work, represent good first-order approximations that are likely to hold at impact and blast strain rates.

The three contexts compared in this paper were: (a) a peak blast overpressure of 5.2 atm corresponding to the Bowen threshold for unarmored lung parenchymal injury; (b) a peak blast overpressure of 18.6 atm corresponding to the Bowen LD_{50} for unarmored lung parenchymal injury; and (c) impact deceleration of the full head model from a velocity of 5 m/s to 0 m/s following impact with a stationary immovable boundary. These conditions were chosen specifically to consider whether there may be calculable evidence for concussive brain injury following primary blast exposure at a specific stand-off. This would appear to be the case under the strict model conditions applied and suggest at a minimum that such a potential threat deserves considered further investigation.

Currently, head PPE tends to be optimized for impact or ballistic protection, with little or no consideration of blast mitigation or protection. The engineering optimization issues required to maximum head PPE should not be underestimated, but consideration of optimizing two domains such as impact and blast injury may be obtainable.

ACKNOWLEDGEMENTS

This work was supported in full by financial aid from the Joint Improvised Explosive Device Defeat Organization (JIEDDO).

References

American Academy of Neurology, 1997: *The Management of Concussion in Sports.*

Belingardi, G., G. Chiandussi, and I. Gaviglio, 2005: Development and validation of a new finite element model of human head. *International Technical Conference on the Enhanced Safety of Vehicles.*

Bowen, I., E. Fletcher, D. Richmond, F. Hirsch, and C. White, 1968: Biophysical mechanisms and scal-

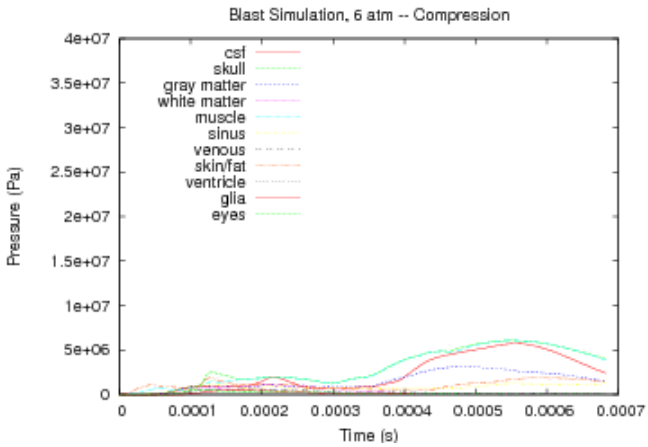

(a) **Compressive Pressure, 5.2 atm**

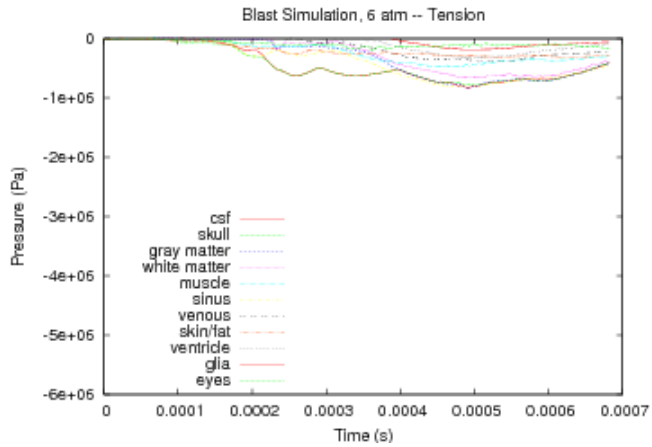

(b) **Tensile Pressure, 5.2 atm**

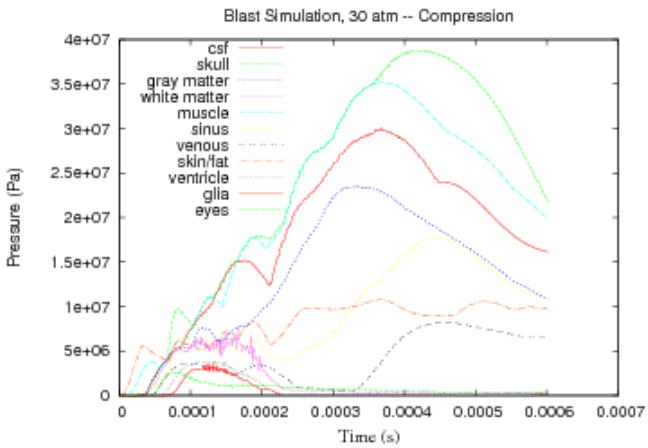

(c) **Compressive Pressure, 18.6 atm**

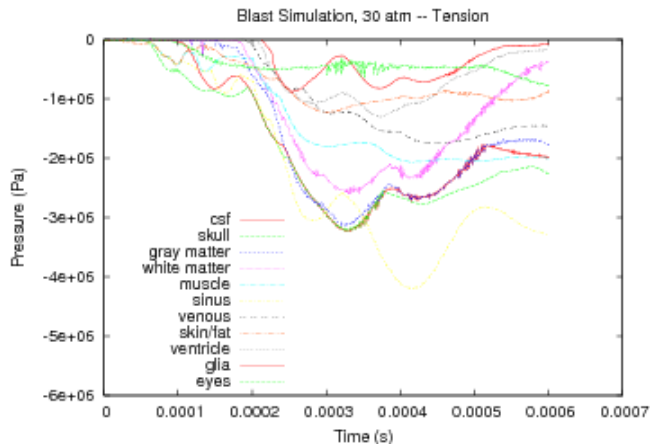

(d) **Tensile Pressure, 18.6 atm**

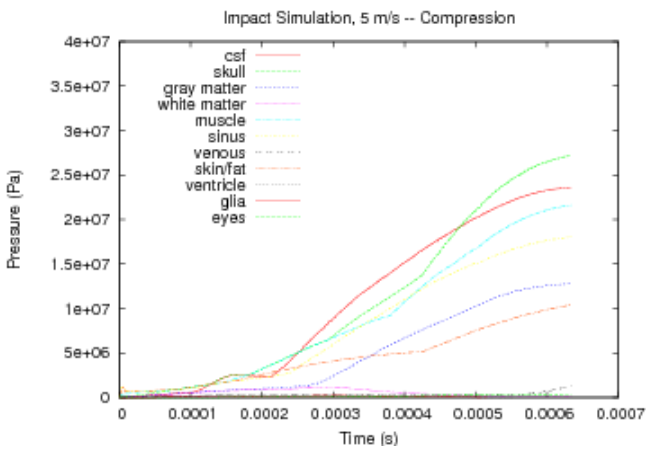

(e) **Compressive Pressure, 5 m/s Impact**

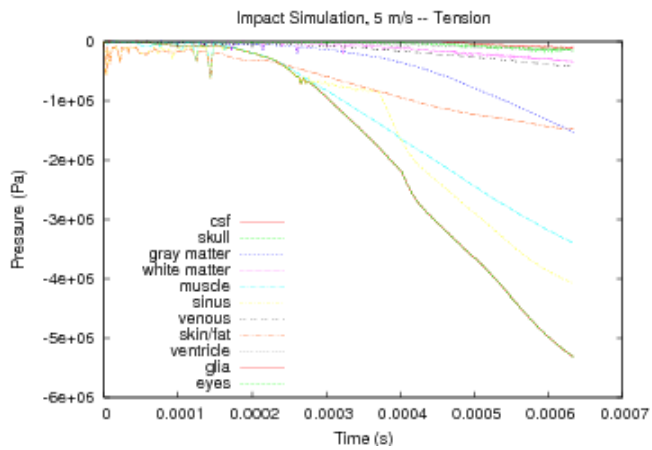

(f) **Tensile Pressure, 5 m/s Impact**

Figure 2: Maximum compressive and tensile pressures reached by differentiated structures in 5.2 atm, 18.6 atm, and 5 m/s impact simulations.

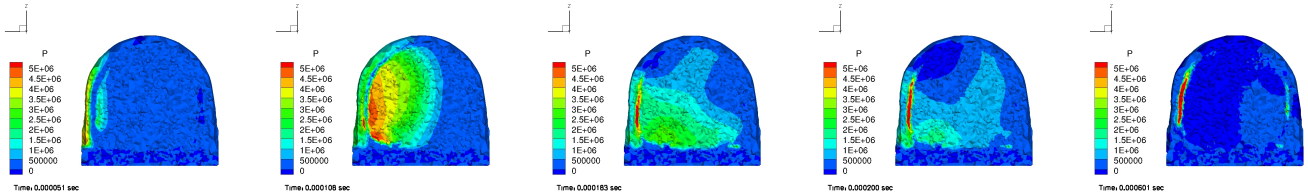

(a) **0.000051 s** (b) **0.000108 s** (c) **0.000183 s** (d) **0.000200 s** (e) **0.000601 s**

Figure 3: Propagation of compressive wave through cranial cavity in 18.6 atm simulation, viewed through mid-coronal plane over a time range of 0.051-0.601 ms. Blast wave is propagated from left to right in the external frame of reference. Scale is from 0 to 5 MPa.

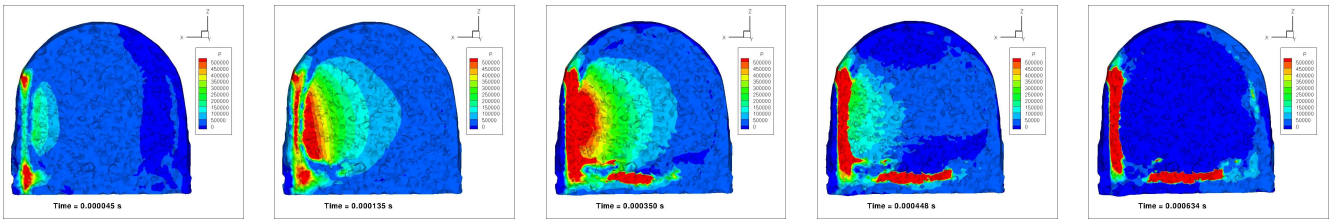

(a) **0.000045 s** (b) **0.000135 s** (c) **0.000350 s** (d) **0.000448 s** (e) **0.000634 s**

Figure 4: Propagation of compressive wave through cranial cavity in 5 m/s impact simulation, viewed through mid-coronal plane

ing procedures applicable in assessing responses of the thorax energized by air-blast overpressures or by nonpenetrating missiles. *Ann N Y Acad Sci*, **152**, 122–146.

Brazarian, J., J. McClung, M. Shah, Y. Cheng, W. Flesher, and J. Kraus, 2005: Mild traumatic brain injury in the united states, 1998-2000. *Brain Injury*, **19**, 85–91.

Bruns, J. and A. Hauser, 2003: The epidemiology of traumatic brain injury: A review. *Epilepsia*, **44**, 2–10.

Casson, I., E. Pellman, and D. Viano, 2008: Concussion in the national football league: An overview for neurologists. *Neurol Clin*, **26**, 217–241.

Collins, D., A. Zijdenbos, V. Kellokian, and et al., 1998: Design and construction of a realistic digital brain phantom. *IEEE T Med Imaging*, **17**, 463–469.

Cullis, I., 2001: Blast waves and how they interact with structures. *J R Army Med Corps*, **147**, 16–26.

Deiterding, R., R. Radovitzky, S. Mauch, L. Noels, J. Cummings, and I. Meiron, 2006: A virtual test facility for the efficient simulation of solid material response under strong shock and detonation wave loading. *Eng Comput*, **22**, 325–344.

D.S. Drumheller, 1998: *Introduction to Wave Propagation in Nonlinear Fluids and Solids*. Cambridge University Press.

Kambouchev, N., R. Radovitzky, and L. Noels, 2007: Fluid-structure interaction effects in the dynamic response of free-standing plates to uniform shock loading. *J Appl Mech*, **74**, 1–5.

Kolsky, H., 1963: *Stress Waves in Solids*. Dover Publications.

M.A. Meyers, 1994: *Dynamic Behavior of Materials*. Wiley Interscience.

Miller, K. and K. Chinzei, 2002: Mechanical properties of brain tissue in tension. *J Biomech*, **35 (4)**, 483–490.

Moore, D., R. Radovitzky, L. Shupenko, A. Klinoff, M. Jaffee, and J. Rosen, 2008: Blast and blast injury of the central nervous system. *Future Neurology*, **3**, 243–250.

Prange, M. and S. Margulies, 2002: Regional, directional, and age-dependent properties of the brain undergoing large deformation. *J Biomech Eng - T ASME*, **124 (2)**, 244–252.

Saraf, H., K. Ramesh, A. Lennon, A. Merkle, and I. Roberts, 2007: Mechanical properties of soft human tissues under dynamic loading. *J Biomech*, **40**, 1960–1967.

Shen, F., T. Tay, J. Li, S. Nigen, P. Lee, and H. Chan, 2006: Modified bilston nonlinear viscoelastic model for finite element head injury studies. *J Biomech Eng - T ASME*, **128 (5)**, 797–801.

Strehlow, R. and W. Baker, 1976: The characterization and evaluation of accidental explosions. *Prog Energ Combust*, **2**, 27–60.

Taylor, G., 1950: The formation of a blast wave by a very intense explosion, II the atomic explosion of 1945. *P Roy Soc A*, **201 (1065)**, 175–186.

Thompson, P., 1972: *Compressible-Fluid Dynamics*. McGraw-Hill.

Velardi, F., F. Fraternali, and M. Angelillo, 2006: Anisotropic constitutive equations and experimental tensile behavior. *Biomech Model Mechan*, **5 (1)**, 1617–7959.

von Neumann, J., 1943: The point source solution. *Collected Works*, Pergamon, Vol. 6, 219–237.

Willinger, R. and D. Baumgartner, 2003: Numerical and physical modelling of the human head under impact – towards new injury criteria. *Int J Vehicle Des*, **32**, 94–115.

Zel'dovich, Y. B. and Y. P. Raizer, 1967: *Physics of Shock Waves and High-Temperature Hydrodynamic Phenomena*, Vol. 2. Academic Press, New York and London.

Zhang, L., K. Yang, and A. King, 2004: A proposed injury threshold for mild traumatic brain injury. *J Biomech Eng - T ASME*, **126 (2)**, 226–236.

Zhang, L., et al., 2001: Recent advances in brain injury research: A new human head model development and validation. *Stapp Car Crash J*, **45**, 369–394.